JOURNAL OF GEOPHYSICAL RESEARCH, VOL. 105, NO. D5, PAGES 6773–6782, MARCH 16, 2000

Stratospheric residence time and its relationship to mean age

Timothy M. Hall

NASA Goddard Institute for Space Studies, New York

Darryn W. Waugh

Department of Earth and Planetary Sciences, Johns Hopkins University, Baltimore, Maryland

Abstract. Transport inaccuracies in stratospheric models are a major source of uncertainty in predicting the environmental impact of trace gases with stratospheric source, such as emissions from high-flying aircraft. Because there are no observed tracers of stratospheric aircraft emissions, a direct evaluation of the models' transport of the emissions is not possible. Here we examine the relationship between the stratospheric residence time τ_R for tracers of midlatitude stratosphere source and the mean age Γ, a transport diagnostic for which observations are available and have been used to evaluate stratospheric models. Employing a representation of the stratosphere that includes the basic kinematic features of the global circulation, we find that τ_R and Γ are correlated over a range of plausible circulations, but that the correlation is imperfect. A major (but not sole) limitation on Γ as a proxy for τ_R is the midlatitude tropopause height Z_M. Elevating Z_M reduces τ_R significantly, while Γ is only weakly affected. The relationship between τ_R and Γ seen among the participants of a recent stratospheric model intercomparison is consistent with this analysis.

1. Introduction

Inaccurate representation of transport in models represents perhaps the greatest uncertainty in assessing the environmental impact of trace gases emitted in the stratosphere, such as those from high-flying aircraft [*Kawa et al.*, 1999]. A recent NASA intercomparison of models and measurements, Models and Measurements II (MMII) [*Park et al.*, 1999], showed large model-to-model differences in simulations of an inert tracer of midlatitude lower stratospheric emissions from such aircraft. To evaluate these simulations, and therefore decide which model predictions are likely most reliable, one would ideally compare the simulations to an observable tracer with similar source (lower stratosphere) and sink (troposphere). Unfortunately, no such tracer is presently observed with sufficient frequency or spatial coverage. There are, however, several quasi-inert tracers of stratospheric transport. The transport information contained by a class of such tracers that have approximately steady tropospheric annually averaged sources and no stratospheric sinks (e.g., CO_2 and SF_6) is summarized by the mean age, $\Gamma(\mathbf{r})$, which is the mean time since air at $\mathbf{r}$ was last in the troposphere [*Hall and Plumb*, 1994]. In recent years, a large number of observational estimates of Γ in the lower and middle stratosphere have been made from airplanes [e.g., *Boering et al.*, 1996; *Elkins et al.*, 1996] and balloons [e.g., *Harnisch et al.*, 1996; *Patra et al.*, 1997]. These observations represent important constraints on model transport.

To take advantage of these constraints, in addition to aircraft emission tracers, the MMII models also simulated the mean age, and these simulations were compared to the observations [*Hall et al.*, 1999]. The models displayed a wide range of mean age distributions, although nearly all were too young compared to observations. It is natural to ask how the observational constraints on modeled mean age apply to modeled stratospheric emissions. One global summary of a stratospheric emission is its residence time, which is the mean over a distribution of transit times for the emission to be transported from its source to the troposphere. Residence time and mean age are deeply related: the mean age at $\mathbf{r}$ in the stratosphere is the residence time for a source at $\mathbf{r}$ in the time-reversed (adjoint) flow (M. Holzer and T. M. Hall, Transit time and tracer age distributions in geophysical flows, submitted to *Journal of Atmospheric Science*, 1999; hereinafter referred to as Holzer and Hall, submitted manuscript, 1999). Moreover, *Boering et al.* [1996] noted that the mean age distribution is equivalent to the steady state response to a uniform source over the stratosphere with a zero tropospheric boundary condition. Thus *Boering et al.* [1996] suggested that mean age may be a good proxy for

Paper number 1999JD901096.
0148-0227/00/1999JD901096$09.00

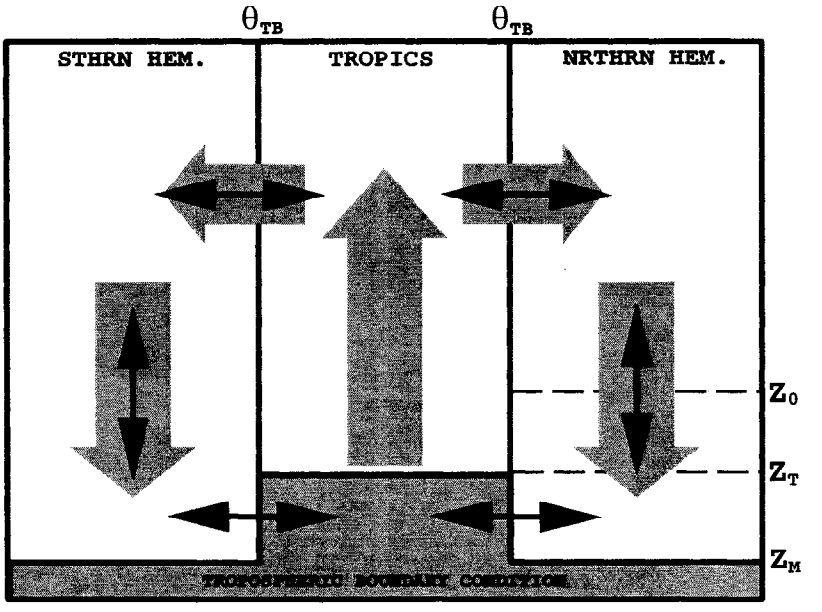

Figure 1. Schematic of the tropical leaky pipe (TLP) model. The stratosphere is divided into three one-dimensional regions representing the tropics and Northern and Southern Hemisphere midlatitude regions, with barrier latitudes as indicated. Vertical advection is upward in the tropics and downward elsewhere (thick shaded vertical arrows). Mass continuity forces a net flux from the tropics to midlatitudes (thick shaded horizontal arrows). This net flux is the difference of gross fluxes in both directions (horizontal double ended arrows). Vertical diffusion occurs in midlatitudes (vertical double ended arrows). The heights of the tropical tropopause, midlatitude tropopause, and Northern Hemisphere tracer source are Z_T, Z_M, and Z_0, respectively. Below the tropopause a tropospheric boundary condition on tracer applies. See text in this paper for details and *Neu and Plumb* [1999] and *Plumb* [1996] for derivation and analysis of the TLP model.

responses to stratospheric emissions, and, consequently, models that underestimate mean age may also underestimate the impact on stratospheric ozone of emissions of stratospheric aircraft.

Long-term stratospheric transport, however, is caused by a variety of dynamical mechanisms, and different diagnostics, such as mean age and residence time, generally weight the mechanisms differently. It is the goal of this paper to analyze in detail the relationship between mean age and the stratospheric residence time of a tracer of midlatitude source. We would like to know with what certainty a model's underestimate of mean age implies an underestimate of residence time. Arguments based on zero- and one-dimensional models of the stratosphere are insufficient, as such models typically have a single transport parameter, and therefore any diagnostic must be perfectly correlated with any other diagnostic as a function of variation in transport. More complexity is necessary to explore differences between mean age and residence time. In complex two- and three-dimensional numerical models, however, it is often difficult to isolate and separate the relative influence of different transport features. In this paper we solve analytically a "tropical leaky pipe" (TLP) model of the stratosphere for a midlatitude lower stratospheric source localized in height, complementing the work of *Neu and Plumb* [1999], who defined, solved and analyzed such a model for the mean age. The TLP model (six parameters, as used in this paper) includes the basic kinematic features of global stratospheric transport but still allows us to interpret simply the impact of these features on mean age and residence time.

2. Tropical Leaky Pipe Model

Neu and Plumb [1999] (hereinafter NP) solved a "tropical leaky pipe" (TLP) model of stratospheric transport to explain features of the mean age distribution present in more complex two-dimensional (2-D) and three-dimensional (3-D) models and in observations. See NP and *Plumb* [1996] for the derivation and discussion of this model. We review the TLP model briefly here, illustrate it schematically in Figure 1, and summarize its variables in Table 1 . The TLP model consists of three coupled one-dimensional (1-D) regions: a "tropical" region with upward advection and Northern and Southern Hemisphere regions (here collectively called "midlatitude" regions) with downward advection. The model formulation is motivated by the many tracer observations that show a tropical region well isolated from the rapid isentropic (quasi-horizontal) mixing of the midlatitude surf zone [e.g., *Trepte and Hitchman*, 1992]. A 1-D representation of tracer transport in the midlatitude regions is justified to the extent that the slope-equilibrium limit applies, in which the tracer isopleths are parallel and their orientations are determined

Table 1. Explanation of Symbols

Symbol	Definition	Type
W	tropical vertical velocity	free parameter
K	midlatitude vertical diffusivity	free parameter
τ	tropical-midlatitude mixing timescale	free parameter
α	tropical to midlatitude air mass ratio	free parameter
Z_T	tropical tropopause height	free parameter
Z_M	midlatitude tropopause height	free parameter
Z_0	midlatitude source height	fixed parameter
H	uniform density scale height	fixed parameter
λ^*	net tropical to midlatitude mass flux rate	constrained
$\epsilon^\#$	net to gross tropical-midlatitude flux ratio	free parameter
τ_R	residence time	computed diagnostic
Γ	mean age	computed diagnostic

* Constrained by mass continuity ($\lambda = \alpha W/H$ for uniform W).

\# Alternative measure of tropical-midlatitude mixing ($\epsilon = \alpha/\tau\lambda$).

purely dynamically by a balance between rapid isentropic mixing and advection by the residual circulation [*Holton*, 1986; *Mahlman et al.*, 1986; *Plumb and Ko*, 1992]. Moreover, in this limit, the isopleths are oriented nearly parallel to isentropes, because isentropic mixing is assumed rapid compared to residual circulation advection.

In addition to advection, the TLP model includes vertical diffusion in midlatitudes, which summarizes the effect of large-scale isentropic mixing in the presence of spatially varying diabatic heating. As discussed by NP, the slope-equilibrium requirement that isopleths are close to isentropes puts an upper bound on vertical diffusion. (NP also include tropical vertical diffusion, which we neglect here for simplicity. Observationally based estimates show vertically diffusive effects to be small in the tropics [*Hall and Waugh*, 1997; *Mote et al.*, 1998].) Finally, the TLP model's tropical and midlatitude regions are coupled. By continuity, the net mass flux from the tropics to midlatitudes ("entrainment flux") is determined by the divergence of the tropical upwelling. However, the gross midlatitude-to-tropical flux ("detrainment flux") is a free parameter, and is summarized here by a time constant τ representing the timescale for tropical tracer values to relax to midlatitude values, an average of the northern and southern hemispheres. The "global diffuser" limit of *Plumb and Ko* [1992], in which there is no isolation of the tropics, corresponds to $\tau = 0$, while the tropical pipe limit of *Plumb* [1996], in which the tropics are perfectly isolated from midlatitudes, corresponds to $\tau = \infty$.

The tropical and midlatitude continuity equations of the TLP model for a tracer of mixing ratio q are

$$\frac{\partial q_T}{\partial t} + W_T \frac{\partial q_T}{\partial Z} = -\frac{1}{\tau}(q_T - q_M) + S_T, \qquad (1)$$

$$\frac{\partial q_{NH}}{\partial t} + W_{NH}\frac{\partial q_{NH}}{\partial Z} - Ke^{Z/H}\frac{\partial}{\partial Z}(e^{-Z/H}\frac{\partial q_{NH}}{\partial Z}) = (\lambda + \frac{\alpha}{\tau})(q_T - q_{NH}) + S_{NH}, \qquad (2)$$

$$\frac{\partial q_{SH}}{\partial t} + W_{SH}\frac{\partial q_{SH}}{\partial Z} - Ke^{Z/H}\frac{\partial}{\partial Z}(e^{-Z/H}\frac{\partial q_{SH}}{\partial Z}) = (\lambda + \frac{\alpha}{\tau})(q_T - q_{SH}) + S_{SH}, \qquad (3)$$

where S is a tracer source, W is vertical velocity, K is the midlatitude vertical diffusivity, H is a constant scale height, $\alpha \equiv M_T/(M_{NH} + M_{SH})$ is the ratio of the tropical to midlatitude atmospheric mass ($\alpha \approx 0.5$ for a tropical barrier at 20°), and λ is the rate at which net entrainment influences midlatitudes. By mass continuity,

$$\lambda = -\alpha e^{Z/H}\frac{\partial}{\partial Z}(e^{-Z/H}W_T(Z)), \qquad (4)$$

which reduces to $\lambda = \alpha W/H$ for spatially uniform W. The vertical coordinate Z is "equivalent height" [*Plumb*, 1996; *Neu and Plumb*, 1999], the height at which a tracer surface intersects the tropical barrier, and tropospheric boundary conditions on q apply at $Z = Z_M$ in midlatitudes and $Z = Z_T$ in the tropics, defining the model's tropopause height in the three regions. The origin $Z = 0$ is arbitrary, and in the solutions Z always appears as $Z - Z_T$ or $Z - Z_M$. The subscripts T, NH, and SH refer to tropics and Northern and Southern Hemisphere extratropics, while the subscript M indicates either extratropical region ("midlatitudes"). Transport in the model is stationary. Therefore, by continuity, downwelling mass flux in midlatitudes must balance the upwelling tropical flux across any level; that is, $W_M(Z) = -\alpha W_T(Z)$. Hereinafter, we write $W_T = W$ and $W_M = -\alpha W$ and assume that $W_{NH} = W_{SH}$. In these equations, K is assumed spatially uniform. An analytic solution is available for spatially varying W for $K = 0$ (see NP for the Γ solution in this case). However, in the following analysis we restrict attention to the case of nonzero K and spatially uniform W. (Note that NP use ϵ as their pipe-diffuser parameter, defined as the ratio of the gross detrainment to the net entrainment, while we often use τ for ease of comparison with observationally based estimates. Comparing our (1) to NP's tropical continuity equation, one

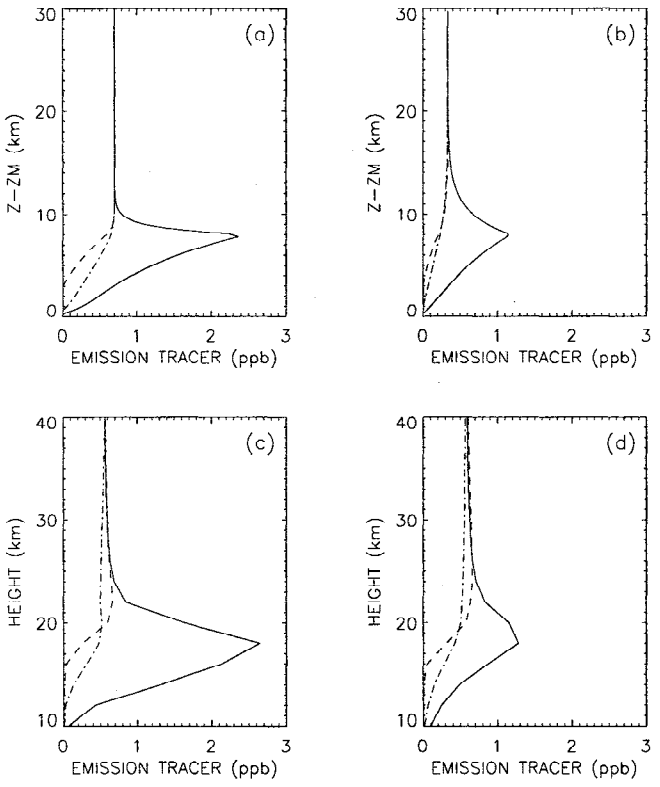

Figure 2. Distributions of an HSCT emission tracer (lower midlatitude stratospheric source, zero tropospheric boundary condition) for (a) the TLP model with $W = 0.25$ mm/s and $K = 0.1$ m^2/s; (b) the TLP model with $W = 0.35$ mm/s and $K = 0.5$ m^2/s; (c) the AER 2-D numerical model [*Ko et al.*, 1985]; and (d) the MONASH1 3-D numerical model [*Rasch et al.*, 1995; *Waugh et al.*, 1997]. For the TLP results in Figures 2a and 2b, $\tau = 0.75$ year, $\alpha = 0.5$ (tropical barrier $\approx 20°$), $Z_T - Z_M = 3$ km, and $Z_0 = 6$ km above Z_M. All TLP profiles are plotted as functions of $Z - Z_M$; that is, height with respect to the midlatitude tropopause. Northern Hemisphere midlatitude profiles are indicated by the solid lines, the tropics by the dashed lines, and the Southern Hemisphere midlatitude by the dot-dash lines. For the numerical models, annual mean results are shown for 45°N (solid line), the equator (dashed line), and 45°S (dot-dash line), and the vertical coordinate is height with respect to the surface, shown above 10 km only. See *Park et al.* [1999] for details on the numerical model experiments.

sees that the two are related simply as $\epsilon = \alpha/(\tau\lambda)$, which reduces to $\epsilon = H/(W\tau)$ for uniform W.)

In summary, the model's free parameters, as used here, are (1) W, the tropical vertical velocity; (2) τ, the timescale for midlatitude air to mix into the tropics; (3) K, the vertical diffusivity in midlatitudes; and (4) α, the measure of the latitude extent of the tropics. Additionally, we consider as free parameters (5) Z_T, and (6) Z_M, the heights of the tropical and midlatitude tropopause. Nonzero $Z_T - Z_M$ represents a "tropopause break" at the bottom of the tropical barrier, allowing tracer in midlatitudes below Z_T to mix directly into the tropical troposphere. These parameters and other variables are listed in Table 1 for convenience.

2.1. Solutions

Analytic steady state solutions to (1), (2), and (3) for mean age and emission tracer are presented in Appendix A for the case of nonzero uniform diffusion and advection. Figure 2 shows two examples of the TLP model's distribution for the parameters $W = 0.25$ mm/s, $K = 0.1$ m^2/s (Figure 2a); and $W = 0.35$ mm/s, $K = 0.5$ m^2/s (Figure 2b). In both cases, $\tau = 0.75$ year, $\alpha = 0.5$ (tropical barrier $\approx 20°$) and $Z_T - Z_M = 3$ km. The source height, Z_0, is 3 km above Z_T (6 km above Z_M). More rapid advection and diffusion as shown in Figure 2b flushes the tracer out of the system more rapidly, so that the steady state value is smaller everywhere.

Also shown in Figure 2 are annual mean profiles from the high-speed civil transport (HSCT) tracer experiment of MMII for the 2-D Atmosphere Environmental Research (AER) model [*Ko et al.*, 1985] and the 3-D chemical transport model (CTM) driven by wind data from the Middle Atmosphere Community Climate Model II (MACCM2) of the National Center for Atmospheric Research [*Rasch et al.*, 1995; *Waugh et al.*, 1997]. (The CTM is called MONASH1, reflecting further development and use at Monash University, Australia.) The MMII experiment specified a constant source of inert HSCT emission tracer concentrated in the Northern Hemisphere and peaking at 18 to 20 km. A zero boundary condition was set in the lower troposphere, and models were run to steady state. (See section 3 and *Park et al.* [1999] for more details on this MMII experiment.) In Figure 2 profiles are shown at 45°S, the equator, and 45°N. The simulated distributions vary widely across the models. For example, the ratio of peak mixing ratio to the mixing ratio at 40 km in northern midlatitudes ranges from 0.10 to 0.64 [*Park et al.*, 1999]. However, certain qualitative characteristics of the simulated distributions are universal. Maximum mixing ratios are found in northern midlatitudes, peaking from 18 to 20 km, the primary source region. Mixing ratios tend toward uniform values aloft. Below the source height the southern midlatitude mixing ratio is greater than the tropical value, while above the source height it is less than the tropical value. AER and MONASH1, whose total stratospheric tracer masses fall near the middle of the MMII range, are plotted in Figure 2 to illustrate these distribution features. Other MMII models would serve equally well. The TLP model captures the qualitative features of the distribution. Quantitative features matching any of the MMII models can be reproduced approximately with suitable TLP parameter values, as is shown for two examples in Figure 2 by comparing Figure 2a with Figure 2c and Figure 2b with Figure 2d.

2.2. Residence Time

A common definition of stratospheric residence time for a tracer in steady state is $\tau_R = M_{SS}/F$, where M_{SS}

is the steady state total tracer mass in the stratosphere and F is the source strength. Although this definition is often practical, and we use it below, it hides an important feature of τ_R. Namely, τ_R in response to a point source at $\mathbf{r}_0$ is a mean over a distribution of transit times from $\mathbf{r}_0$ to the tropopause, just as $\Gamma(\mathbf{r})$ is the mean over a distribution of transit times from the tropopause to $\mathbf{r}$. The equivalence between this distribution mean and M_{SS}/F is derived in Appendix B.

Using the solutions (A3), (A4), and (A5), we calculate the residence time to be

$$\tau_R = \frac{H}{K(1+H/h)}\Big((1+\epsilon\tilde{\alpha})(Z_0-Z_M) - \tilde{\alpha}\epsilon H(e^{\Delta Z/H}-1)+\tilde{\alpha}\epsilon h(1-e^{-\Delta Z/h})\Big), \quad (5)$$

where $h^{-1} = (W/K)(\alpha + (\epsilon K/WH))$, $\tilde{\alpha} = 1+\alpha$, Z_0 is the height of the Northern Hemisphere midlatitude source, $\Delta Z = Z_T - Z_M$, and Z_T and Z_M are the heights of the tropical and midlatitude (north and south) tropopauses. It is worthwhile pointing out a limiting case. For $Z_T = Z_M$ (causing the second two terms on the right-hand side of (5) to vanish) and low diffusion ($K \to 0$),

$$\tau_R \sim (1+\epsilon+\alpha\epsilon)\frac{(Z_0-Z_M)}{\alpha W}. \quad (6)$$

The factor $\tau_W \equiv (Z_0 - Z_M)/(\alpha W)$ is the timescale for advection in midlatitudes to carry tracer from the source down to the tropopause, and the factor $A \equiv 1+\epsilon+\alpha\epsilon$ represents the amplification of τ_W due to recirculation when the tropics are not perfectly isolated ($\epsilon > 0$). Substituting $\epsilon = H/W\tau$ and considering the simplest case of equal mass tropics and midlatitudes ($\alpha = 1$), one sees that the amplification of τ_R due to recirculation is $A = 1 + (2H/W)(\tau_W/\tau)$. Evidently, recirculation contributes the time $2H/W$ to travel up and back down a scale height, adjusted by the fraction τ_W/τ of tracer that "leaks" into the tropics before exiting through the midlatitude tropopause.

If $Z_T > Z_M$ then tracer in midlatitudes below Z_T can mix straight into the tropical troposphere where it is removed and therefore not available for recirculation. The second term on the right-hand side of (5) represents the reduction of τ_R due to this process. However, midlatitude tracer below Z_T can escape the mixing into the tropical troposphere by diffusing upwards above Z_T. This possibility is represented by the third term on the right-hand side of (5), which moderates the reduction of τ_R by the second term. For $K \to 0$, the third term vanishes.

Expressions (5), (A1), and (A2) show that τ_R and Γ do not depend on the circulation parameters in the same way. To illustrate the relative sensitivities, we plot in Figure 3a τ_R versus $\Gamma_M(Z_0)$ (midlatitude mean age evaluated at the source height) for a northern midlatitude source. We vary W, K, τ, and α one at a time over the ranges $W = 0.25 \to 0.35$ mm/s, $K = 0.01 \to 0.3$ m^2/s, $\tau = 0.75 \to 1.5$ year, and $\alpha = 0.35 \to 0.73$ (equivalent to tropical barrier latitude from 15° to 25°). For each variation the constant parameters are held at the midpoints of their ranges. These parameter ranges loosely bracket the ranges of values inferred from observations [*Volk et al.*, 1996; *Boering et al.*, 1996; *Hall and Waugh*, 1997; *Sparling et al.*, 1997; *Mote et al.*, 1998; *Grant et al.*, 1996]. Both τ_R and $\Gamma_M(Z_0)$ decrease with increasing W and K (more rapid circulation through the system), decrease with increasing τ (less recirculation), and decrease with increasing α (less massive midlatitudes requiring more rapid downwelling by continuity). Similar sensitivities are found for Γ_T (not shown).

Figure 3a also shows the τ_R and $\Gamma_M(Z_0)$ sensitivity to Z_M and Z_T. In the first case we raise Z_M from $Z_0 - 6$ km to $Z_0 - 3$ km, holding Z_T fixed at $Z_0 - 3$ km. In the second case we raise Z_T from $Z_0 - 4.5$ km to $Z_0 - 3$ km holding Z_M fixed at $Z_0 - 4.5$ km. Raising Z_M provides a shorter path to first contact with the tropopause from Z_0 and therefore a reduced τ_R. On the other hand, $\Gamma_M(Z_0)$ depends on the transit times since last contact with the tropopause, which occurs primarily in the tropics. Therefore $\Gamma_M(Z_0)$ depends only weakly on Z_M. (The Γ_M dependence on Z_M is due to the small diffusive contact with the midlatitude tropopause. For $K = 0$, Γ_M is completely independent of Z_M, and $\Gamma_M > 0$ down to Z_M, at which point it changes discontinuously to zero. Small K provides a shallow boundary layer of depth $K/(\alpha W)$ over which Γ_M approaches zero continuously. See NP for further discussion.) The differing sensitivity of τ_R and Γ_M to Z_M is the major reason in the TLP model for the imprecision of Γ as a proxy for τ_R. In contrast to Z_M, raising Z_T reduces both timescales roughly equivalently by providing a shorter path since last tropical tropopause contact (reducing Γ_M) and a larger region in mixing contact with the tropical troposphere (reducing τ_R).

While τ_R and Γ depend on the model parameters with the same sign, they have different sensitivities. Therefore varying all the model parameters simultaneously results in a noncompact scatterplot. This is shown in Figure 3b for the same range of parameter values as in Figure 3a. The scatterplot τ_R versus $\Gamma_M(Z_0)$ is shown in gray and τ_R versus $\Gamma_T(Z_0 + 3$ km) is shown in black. In the figure each point can be considered as a possible "stratospheric circulation." The large range of τ_R and Γ indicates the high sensitivity of these timescales as transport diagnostics. Without any additional information, an observation of Γ constrains τ_R to a range of values. For example, $\Gamma_M(Z_0) = 3.0$ years implies τ_R between 1.1 and 2.1 years. Thus, if a stratospheric model simulated the values $\Gamma_M(Z_0) = 2.5$ years and $\tau_R = 1.5$ years, it would underestimate the mean age, but its τ_R could either be an underestimate or an overestimate of the true residence time. The range on τ_R implied by the Γ observation would be larger or smaller for larger or smaller bounds on the circulation parameters. Note also that the line of best fit through the (Γ, τ_R) points is not $\tau_R = \Gamma$. The slope and intercept of the line varies with evaluation point of Γ and source height Z_0.

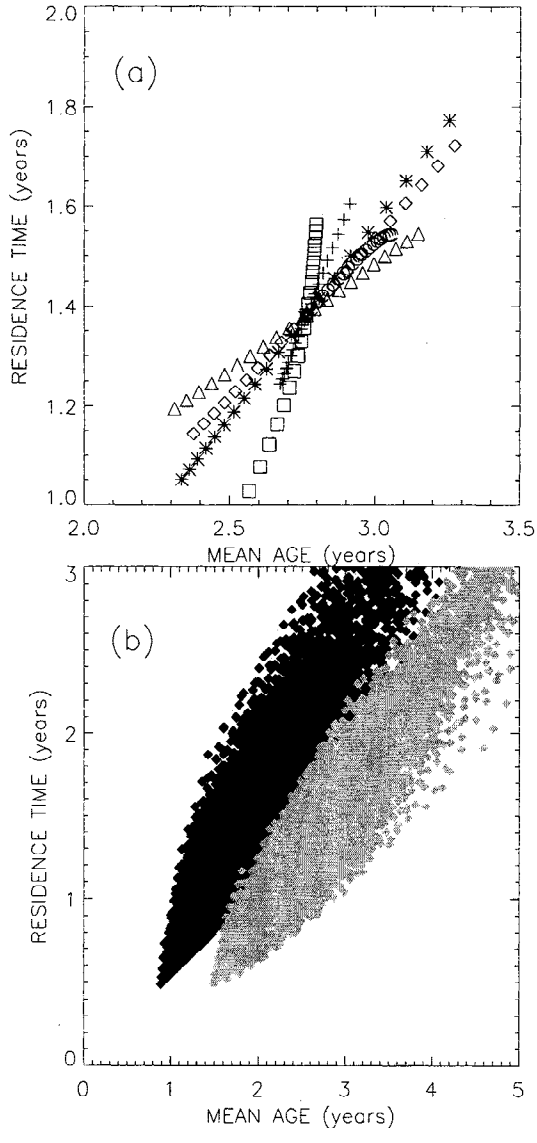

Figure 3. (a) Scatterplot of TLP τ_R versus Γ_M with model parameters varied one by one. Γ_M is evaluated at Z_0. The parameter ranges are $W = 0.25 \rightarrow 0.35$ mm/s (diamonds); $K = 0.01 \rightarrow 0.3$ m^2/s (triangles); $\tau = 0.75 \rightarrow 1.5$ years (crosses); $\alpha = 0.35 \rightarrow 0.73$ (asterisks, equivalent to tropical barrier latitude from 15° to 25°); $Z_M = Z_0 - 6$ km $\rightarrow Z_0 - 3$ km with $Z_T = Z_0 - 3$ km (squares); and $Z_T = Z_0 - 4.5$ km $\rightarrow Z_0 - 3$ km with $Z_M = Z_0 - 4.5$ km (circles). In all cases the direction of increasing parameter value is toward decreasing τ_R and Γ_M. (b) All parameters varied simultaneously over the same range as in Figure 3a. Shaded symbols indicate Γ_M evaluated at Z_0 as in Figure 3a, and black symbols indicate Γ_T evaluated at $Z_0 + 3$ km. Note that the scale in Figure 3b is expanded compared to Figure 3a.

3. MMII Models

As part of MMII, an inert tracer of emissions from HSCT was defined, which had a steady source concentrated in the lower stratosphere at northern midlatitudes and a zero boundary condition in the lower troposphere. Both 2-D and 3-D models performed the experiment. Examples of annual mean profiles of the mixing ratio resulting from this HSCT experiment are shown in Figure 2 for two of the models. There are large differences among the models' distributions. For example, total tracer mass above 16 km varies by roughly a factor 4 across the models, while the northern to southern hemispheric ratio varies by a factor 3. See *Park et al.* [1999] for more details and complete model descriptions.

Figure 4 shows the residence time versus mean age for most of the MMII models. The numbers in the symbols indicate the model according to Table 2 of *Hall et al.* [1999]. Open symbols represent 2-D models, and shaded symbols represent 3-D. The AER and MONASH1 models shown in Figure 2 correspond to symbols 1 and 18, respectively. We compute τ_R as the total tracer mass above the tropopause divided by the source strength. The tropopause is defined as the height at which N_2O falls to 98% of its surface mixing ratio for each model. In this figure Γ is evaluated at 50°N and 20 km in pressure altitude (selected to represent the midlatitude lower stratosphere) and is referenced to the value at a model's tropical tropopause. We have found that other definitions of τ_R (for example, using tracer mass above the 100 mbar level) and evaluation points for Γ yield qualitatively similar relationships between τ_R and Γ across the models.

The large range of τ_R and Γ simulated by the MMII models is apparent in Figure 4. As discussed by *Hall et al.* [1999], most MMII models underestimate Γ,

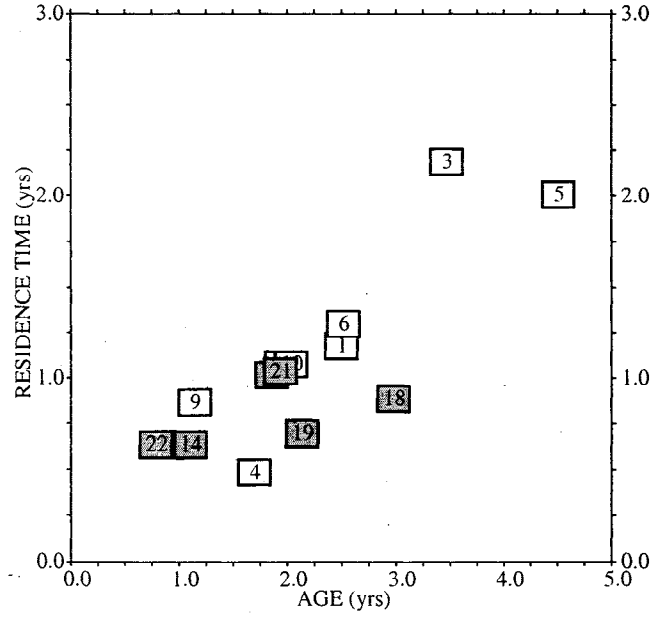

Figure 4. Scatterplot of TLP τ_R versus Γ_M across the MMII models. Each symbol is a result from a different MMII model, numbered according to Table 2 of *Hall et al.* [1999]. Open symbols represent 2-D models, and shaded symbols represent 3-D models. The AER and MONASH1 models shown in Figure 2 correspond to symbols 1 and 18, respectively. Γ_M is evaluated at 50°N and 20 km in pressure altitude. See *Park et al.* [1999] for details on the experiment and the models.

which observations show to be 3.5 to 4.5 years at this latitude and height (e.g., Figure 5 of *Hall et al.* [1999]). There is a correlation between τ_R and Γ across the models, but it is imperfect. For example, for $\Gamma = 2$ years, τ_R varies from about 0.6 to 1.1 years. The scatter is somewhat larger than the TLP result of Figure 3b. The MMII models' circulations vary more widely than the parameter ranges of Figure 3b, which are based on observations; the source functions vary somewhat from model to model depending on resolution; and the MMII models include processes not represented by the TLP model. Overall, the MMII results reinforce the conclusion from the TLP analysis that mean age is only an imperfect constraint on residence time. Note that τ_R and Γ are most differently sensitive to variations in the height of the midlatitude tropopause, as seen in Figure 3a. Across the MMII models plotted here, the midlatitude tropopause, defined by 98% surface N_2O at the latitude of peak emission tracer mixing ratio, varies from 8.1 to 12.6 km.

There is a weak tendency for 3-D models to have smaller τ_R than 2-D models for the same Γ. The difference between 2-D and 3-D is more pronounced upon comparing Γ directly to the mixing ratio of emission tracer at and near the source (see *Park et al.* [1999, Figure 42, chapter 2] and *Kawa et al.* [1999, Figure 4-15]), while elsewhere there is little distinction. The reasons for this difference are uncertain, but it is consistent with a weak tendency for N_2O in the MMII 3-D models to change more gradually across the midlatitude tropopause than in the 2-D models, suggesting more mixing between the lower stratosphere and upper troposphere in 3-D. *Rasch et al.* [1994] discussed a similar emission tracer difference between 2-D and 3-D. We emphasize, however, that the differences among 3-D MMII models and among 2-D MMII models is greater than the difference between the groups.

4. Summary and Discussion

The residence time τ_R is the mean of a distribution of transit times for air and tracer in a stratospheric source region to make first contact with the troposphere and is one measure of the role of transport in determining the environmental effects of trace gases of stratospheric source, such as those from high-flying aircraft. Unfortunately, τ_R is not observable directly. In this paper we have used a simple model of stratospheric transport to understand and quantify the relationship between τ_R and the mean age Γ for which extensive observations are available in the lower stratosphere. Our goal has been to determine the extent to which Γ is a proxy for τ_R, and the extent to which a stratospheric model's error in Γ implies a commensurate error in τ_R.

A "tropical leaky pipe" model of stratospheric transport similar to that employed to study mean age by *Neu and Plumb* [1999] serves us well for this purpose, as it offers enough complexity to explore realistically differences between τ_R and Γ, yet is simple enough to allow easy interpretation. The model includes representations of the basic features of the global, time-averaged stratospheric circulation. We find that τ_R and Γ depend on the magnitudes of these circulation features with the same sign but differing sensitivity. Thus when all model parameters are varied simultaneously over ranges roughly bracketing observational estimates, τ_R and Γ are correlated, but there is significant scatter. For example, $\Gamma = 3$ years in the midlatitude stratosphere at the height of the emission tracer source constrains τ_R to the approximate range 1.1 to 2.1 years. For a source in the lower midlatitude stratosphere the circulation feature that affects τ_R and Γ most differently is the height Z_M of the midlatitude tropopause. An elevated Z_M significantly reduces τ_R, as it shortens the direct transport path from the source to the troposphere, but it has little impact on Γ, which is sensitive to pathways from the tropical tropopause.

The relationship between residence time and mean age impacts the role of mean age in evaluating models used to assess the environmental effects of stratospheric aircraft. Nearly all the stratospheric models (2-D and 3-D) that participated in MMII underestimate Γ compared to observations [*Hall et al.*, 1999]. A model that grossly underestimates Γ likely also underestimates the stratospheric residence time τ_R of HSCT emissions, while a model that only moderately underestimates Γ could moderately underestimate or overestimate τ_R. It is clear that transport inaccuracies in these models are a primary source of assessment uncertainty [*Kawa et al.*, 1999]. While mean age provides an important evaluation tool, additional tracers are necessary to constrain more completely the models' transport of stratospheric emissions, such as those from aircraft. Ideally, such tracers would be inert in the stratosphere and have stratospheric source and tropospheric sink. The isotopic constituent ^{14}CO [*Mak and Southon*, 1998; *Jockel et al.*, 1999], the isotopic ratio $^{10}Be/^{7}Be$ [*Koch and Rind*, 1998], and the stratospheric-generated anomaly of the isotopic mass ratio $^{17}O/^{18}O$ [*Luz et al.*, 1999] are possible candidates.

Appendix A: Solutions to the Tropical Leaky Pipe Model

The mean age is the lag time for a tracer of linearly increasing tropospheric abundance [*Hall and Prather*, 1993]. Equations of motion for the mean age are obtained most conveniently for the TLP model by substituting $q(Z,t) = q(0, t - \Gamma(Z)) \propto t - \Gamma(Z)$ into (1), (2), and (3); setting $S_{NH} = S_T = S_{SH} = 0$; applying the boundary conditions $\Gamma_T(Z_T) = \Gamma_M(Z_M) = 0$, and considering steady state. The linear increase in tracer acts as an effective uniform unit source for Γ. The Γ equations are discussed and solved in this fashion by NP. Note that NP include vertical diffusion in midlatitudes, which we neglect here. We consider the case of uniform and constant coefficients. (Analytic solutions are also available for spatially varying W when $K = 0$, as discussed by NP.) The resulting equations can be solved

simultaneously using standard methods. We find for mean age

$$\Gamma_T(Z) = b(Z - Z_T) - ah(e^{-(Z-Z_M)/h} - e^{-\Delta Z/h}), \quad \text{(A1)}$$

$$\Gamma_M(Z) = b(Z - Z_T) - ah(e^{-(Z-Z_M)/h} - e^{-\Delta Z/h}) + a\frac{H}{\epsilon}e^{-(Z-Z_M)/h} + \frac{H}{\epsilon W}(bW - 1), \quad \text{(A2)}$$

where

$$a = \frac{\alpha - b\alpha W + b\epsilon\lambda\Delta Z}{\alpha W + \epsilon\lambda h(e^{-\Delta Z/h} - 1)},$$

$$b = \frac{\epsilon + \alpha(1+\epsilon)}{\alpha W + \epsilon K/H},$$

$$h^{-1} = \frac{W}{K}(\alpha + \frac{\epsilon K}{WH}),$$

and where $\Delta Z = Z_T - Z_M$ and $\lambda = \alpha W/H$.

The equations of motion for $q(Z)$, the mixing ratio response to a constant midlatitude point source at Z_0, are obtained by substituting into (1), (2), and (3) the sources $S_{SH} = S_T = 0$ and $S_{NH} = F\delta(Z - Z_0)/\rho(Z_0)$, where F is the source strength (mass/time) and ρ is the 1-D air mass density. The boundary conditions are $q_T(Z_T) = q_M(Z_M) = 0$, and we consider steady state. The resulting equations can be solved by first decoupling the three regions, then obtaining general solutions above and below Z_0 separately, and finally applying the boundary conditions and the condition of continuity across Z_0 to constrain general constants. For $K = 0$ this can be done for general spatial variation in W. However, we restrict attention to nonzero K and uniform W, finding

$$q_T(Z) = \epsilon Q \begin{cases} \frac{h}{H}(e^{\tilde{Z}_0/H} - e^{-\Delta Z/h}) \\ \quad -\frac{h}{H}(e^{\tilde{Z}_0/h}e^{\tilde{Z}_0/H} - 1)e^{-\tilde{Z}/h} \\ \quad +(e^{\tilde{Z}_0/H} - e^{\Delta Z/H}), & Z > Z_0 \\ \\ -\frac{h}{H}(e^{-\Delta Z/h} - e^{-\tilde{Z}/h}) \\ \quad (e^{\tilde{Z}/H} - e^{\Delta Z/H}), & Z < Z_0, \end{cases} \quad \text{(A3)}$$

$$q_{NH}(Z) = \frac{1}{2}(q_+ + q_-), \quad \text{(A4)}$$

$$q_{SH}(Z) = \frac{1}{2}(q_+ - q_-), \quad \text{(A5)}$$

where

$$q_+(\tilde{Z}) = Q \begin{cases} (1 - \epsilon\frac{h}{H})(e^{\tilde{Z}_0/h}e^{\tilde{Z}_0/H} - 1)e^{-\tilde{Z}/h} \\ \quad +\epsilon(e^{\tilde{Z}_0/H} - e^{\Delta Z/H}) \\ \quad +\epsilon\frac{h}{H}(e^{\tilde{Z}_0/H} - e^{-\Delta Z/h}), & Z > Z_0 \\ \\ (e^{\tilde{Z}/H} - e^{-\tilde{Z}/h}) \\ \quad +\epsilon(e^{\tilde{Z}/H} - e^{\Delta Z/H}) \\ \quad -\epsilon\frac{h}{H}(e^{-\Delta Z/h} - e^{-\tilde{Z}/h}), & Z < Z_0, \end{cases}$$

$$q_-(Z) = \frac{F}{2K(\gamma_+ - \gamma_-)}e^{\tilde{Z}_0/H}(e^{-\gamma_-\tilde{Z}_0} - e^{-\gamma_+\tilde{Z}_0}) \times \begin{cases} e^{\gamma_-\tilde{Z}}, & Z > Z_0 \\ e^{\gamma_-\tilde{Z}_0}\left(\frac{e^{\gamma_-\tilde{Z}} - e^{\gamma_+\tilde{Z}}}{e^{\gamma_-\tilde{Z}_0} - e^{\gamma_+\tilde{Z}_0}}\right), & Z < Z_0, \end{cases}$$

$$\gamma_\pm = (\frac{1}{2H} - \frac{\alpha W}{2K}) \pm \sqrt{(\frac{1}{2H} + \frac{\alpha W}{2K})^2 + \frac{\alpha}{K\tau}},$$

$$Q = \frac{FH}{2K(1 + \frac{H}{h})},$$

and where $\tilde{Z} \equiv Z - Z_M$, $\tilde{Z}_0 \equiv Z_0 - Z_M$, and $\Delta Z \equiv Z_T - Z_M$. Expressions (A3), (A4), and (A5) are integrated over the domain (mass weighted) and divided by the source strength F to obtain expression (5) for the residence time.

Appendix B: Residence Time as a Mean of a Distribution

The Green function $G(\mathbf{r}, t|\mathbf{r}_0, t_0)$ is the mixing ratio response to an instantaneous unit tracer source at $\mathbf{r}_0$ and t_0 in a reservoir R. A zero mixing ratio condition is applied on some region Ω of the reservoir boundary, and zero flux conditions on all other regions. As time passes tracer leaks out of the reservoir through contact with Ω. The total tracer mass M remaining in R after elapsed time ξ is

$$M(t_0 + \xi|\mathbf{r}_0, t_0) = \int_R \rho(\mathbf{r})G(\mathbf{r}, t_0 + \xi|\mathbf{r}_0, t_0)d\mathbf{r}, \quad \text{(B1)}$$

where ρ is the fluid mass density. M may also be interpreted as the probability that a fluid "particle" (infinitesimal material element) labeled by tracer at $\mathbf{r}_0$ and t_0 has not yet made contact with Ω after transit time ξ. The probability density function for particles to make first contact with Ω at ξ is proportional to the flux of tracer mass out of R; that is, the probability that a particle makes first contact with Ω in the transit time range $\xi \to \xi + \delta\xi$ is $-\delta\xi\frac{\partial}{\partial\xi}M(t_0 + \xi|r_0, t_0)$ (Holzer and Hall, submitted manuscript, 1999). The mean transit time to first contact $\bar{\xi}$ is therefore

$$\bar{\xi}(\mathbf{r}_0, t_0) = -\int_0^\infty \xi\frac{\partial}{\partial\xi}M(t_0 + \xi|\mathbf{r}_0, t_0)d\xi. \quad \text{(B2)}$$

Assuming sufficient M convergence with ξ, (B2) becomes

$$\bar{\xi}(\mathbf{r}_0, t_0) = \int_0^\infty M(t_0 + \xi|\mathbf{r}_0, t_0)d\xi. \quad \text{(B3)}$$

The "residence time" τ_R is defined as M_{SS}/F (called the "turnover time" by *Bolin and Rhode* [1973]), where M_{SS} is the steady state total mass in R in response to a constant input flux $F(t) = F$ at $\mathbf{r}_0$. By the property of

the Green function the response $\chi(\mathbf{r},t)$ to the constant source is

$$\chi(\mathbf{r},t) = \int_{-\infty}^{t} F(t_0)G(\mathbf{r},t|\mathbf{r}_0,t_0)dt_0 = F\int_0^{\infty} G(\mathbf{r},t|\mathbf{r}_0,t-\xi)d\xi, \quad \text{(B4)}$$

where ξ is the elapsed time $t-t_0$ since the steady source was turned on. Using (B1) and (B4) the total mass $M_{SS} = \int_R \rho(\mathbf{r})\chi(\mathbf{r},t)d\mathbf{r}$ is

$$M_{SS}(t,\mathbf{r}_0) = F\int_0^{\infty} M(t|\mathbf{r}_0,t-\xi)d\xi. \quad \text{(B5)}$$

Comparison of (B3) and (B5) shows that if transport is stationary then

$$\tau_R = \frac{M_{SS}}{F} = \bar{\xi}. \quad \text{(B6)}$$

Acknowledgments. We thank the participants of the Models and Measurements II study for their efforts and for making available their model data, in particular, Malcolm Ko for the AER result shown in Figure 2. Alan Plumb contributed significantly to improvements on an early draft of the manuscript. We also thank David Rind for helpful comments. Finally, we thank Steve Wofsy for conversations that motivated this study. This work is supported by the NASA Atmospheric Effects of Aviation Program project NAG5-7138.

References

Boering, K. A., S. C. Wofsy, B. C. Daube, H. R. Schneider, M. Loewenstein, and J. R. Podolske, Sratospheric mean ages and transport rates derived from observations of CO_2 and N_2O, *Science*, *274*, 1340–1343, 1996.

Bolin, B., and H. Rhode, A note on the concepts of age distribution and transit time in natural reservoirs, *Tellus*, *25*, 58–62, 1973.

Elkins, J. W., et al., Airborne gas chromatograph for in situ measurements of long-lived species in the upper troposphere and lower stratosphere, *Geophys. Res. Lett.*, *23*, 347–350, 1996.

Grant, W. B., E. V. Browell, C. S. Long, L. L. Stowe, R. G. Grainger, and A. Lambert, Use of volcanic aerosols to study the tropical stratospheric reservoir, *J. Geophys. Res.*, *101*, 3973–3988, 1996.

Hall, T. M., and R. A. Plumb, Age as a diagnostic of stratospheric transport, *J. Geophys. Res.*, *99*, 1059–1070, 1994.

Hall, T. M., and M. J. Prather, Simulations of the trend and annual cycle in stratospheric CO_2, *J. Geophys. Res.*, *98*, 10,573–10,581, 1993.

Hall, T. M., and D. W. Waugh, Tracer transport in the tropical stratosphere due to vertical diffusion and horizontal mixing, *Geophys. Res. Lett.*, *24*, 1383–1386, 1997.

Hall, T. M., D. W. Waugh, K. A. Boering, and R. A. Plumb, Evaluation of transport in stratospheric models, *J. Geophys. Res.*, *104*, 18,815–18,839, 1999.

Harnisch, J., R. Borchers, P. Fabian, and M. Maiss, Tropospheric trends for CF_4 and C_2F_6 since 1982 derived from SF_6 dated stratospheric air, *Geophys. Res. Lett.*, *23*, 1099–1102, 1996.

Holton, J. R., A dynamically based transport parameterization for one-dimensional photochemical models of the stratosphere, *J. Geophys. Res.*, *91*, 2681–2686, 1986.

Jockel, P., M. G. Lawrence, and C. A. M. Brenninkmeijer, Simulations of cosmogenic ^{14}CO using the three-dimensional atmospheric model MATCH: Effects of ^{14}CO production distribution and the solar cycle, *J. Geophys. Res.*, *104*, 11,733–11,743, 1999.

Kawa, S. R., et al., Assessment of the effects of high-speed aircraft in the stratosphere: 1998, *NASA Tech. Publ.*, *NASA/TP-99-209236*, 1999.

Ko, M. K. W., K. K. Tung, D. K. Weisenstein, and N. D. Sze, A zonal mean model of stratospheric tracer transport in isentropic coordinates: Numerical simulations for nitrous oxide and nitric acid, *J. Geophys. Res.*, *90*, 2313–2329, 1985.

Koch, D., and D. Rind, Beryllium 10/beryllium 7 as a tracer of stratospheric transport, *J. Geophys. Res.*, *103*, 3907–3917, 1998.

Luz, B., E. Barkan, M. L. Bender, K. H. Thiemens, and K. A. Boering, Triple-isotope composition of atmospheric oxygen as a tracer of biospheric productivity, *Nature*, *400*, 547–550, 1999.

Mahlman, J. D., H. Levy, and W. J. Moxim, Three-dimensional simulations of stratospheric N_2O: Predictions for other trace constituents, *J. Geophys. Res.*, *91*, 2687–2707, 1986.

Mak, J. E., and J. R. Southon, Assessment of tropical OH seasonality using atmospheric ^{14}CO measurements from Barbados, *Geophys. Res. Lett.*, *25*, 2801–2804, 1998.

Mote, P. W., T. J. Dunkerton, M. E. McIntyre, E. A. Ray, and P. H. Haynes, Vertical velocity, vertical diffusion, and dilution by midlatitude air in the tropical lower stratosphere, *J. Geophys. Res.*, *103*, 8651–8666, 1998.

Neu, J. L., and R. A. Plumb, The age of air in a leaky pipe model of stratospheric transport, *J. Geophys. Res.*, *104*, 19,243–19,255, 1999.

Park, J., M. K. W. Ko, R. A. Plumb, C. H. Jackman, J. A. Kaye, and K. H. Sage, Report of the 1998 Models and Measurements II Workshop, *NASA Tech. Publ.*, *NASA/TM-1999-209554*, 1999.

Patra, P. K., S. Lal, B. H. Subbaraya, C. H. Jackman, and P. Rajaratnam, Observed vertical profile of sulphur hexafluoride (SF_6) and its atmospheric applications, *J. Geophys. Res.*, *102*, 8855–8859, 1997.

Plumb, R. A., A tropical pipe model of stratospheric transport, *J. Geophys. Res.*, *101*, 3957–3972, 1996.

Plumb, R. A., and M. K. W. Ko, Interrelationships between mixing ratios of long-lived stratospheric constituents, *J. Geophys. Res.*, *97*, 10,145–10,156, 1992.

Rasch, P. J., X. Tie, B. A. Boville, and D. L. Williamson, A three-dimensional transport model for the middle atmosphere, *J. Geophys. Res.*, *99*, 999–1017, 1994.

Rasch, P. J., B. A. Boville, and G. P. Brasseur, A three-dimensional general circulation model with coupled chemistry for the middle atmosphere, *J. Geophys. Res.*, *100*, 9041–9071, 1995.

Sparling, L. C., J. A. Kettleborough, P. H. Haynes, M. E. McIntyre, J. E. Rosenfield, M. R. Schoeberl, and P. A. Newman, Diabatic cross-isentropic dispersion in the lower stratosphere, *J. Geophys. Res.*, *102*, 25,817–25,829, 1997.

Trepte, C. R., and M. H. Hitchman, Tropical stratospheric circulation deduced from satellite aerosol data, *Nature*, *355*, 626–628, 1992.

Volk, C. M., et al., Quantifying transport between the tropical and mid-latitude lower stratosphere, *Science*, *272*, 1763–1768, 1996.

Waugh, D. W., et al., Three-dimensional simulations of long-lived tracers using winds from MACCM2, *J. Geophys. Res.*, *102*, 21,493–21,513, 1997.

T. M. Hall, NASA Goddard Institute for Space Studies, 2880 Broadway, New York, NY 10025. (thall@giss.nasa.gov)

D. W. Waugh, Department of Earth and Planetary Science, Johns Hopkins University, 3400 N. Charles St., Baltimore, MD 21218. (waugh@jhu.edu)

(Received September 10, 1999; revised October 21, 1999; accepted October 25, 1999.)